DOI:
10.1016/j.commatsci.2020.110140

Document Version
Peer reviewed version

Efficient magnetic superstructure optimization with ΘΦ

Evgeny A. Plekhanov[1,2,*] and Andrei L. Tchougréeff[2]

[1] *King's College London, Theory and Simulation of Condensed Matter (TSCM), The Strand, London WC2R 2LS, UK*
[2] *A.N. Frumkin Institute of Physical Chemistry and Electrochemistry of RAS, Moscow, Russia*

(Dated: November 23, 2020)

Simulating the incommensurate spin density waves (ISDW) states is not a simple task within the standard *ab-initio* methods. Moreover, in the context of new material discovery, there is a need for fast and reliable tool capable to scan and optimize the total energy as a function of the pitch vector, thus allowing to automatize the search for new materials. In this paper we show how the ISDW can be efficiently obtained within the recently released ΘΦ program. We illustrate this on an example of the single orbital Hubbard model and of γ-Fe, where the ISDW emerge within the mean-field approximation and by using the twisted boundary conditions. We show the excellent agreement of the ΘΦ with the previously published ones and discuss possible extensions. Finally, we generalize the previously given framework for spin quantization axis rotation to the most general case of spin-dependent hopping matrix elements.

Keywords: Hubbard model, Heisenberg model, spin-density waves, strongly-correlated systems

INTRODUCTION

Incommensurate spin structures (ISS) appear in various contexts of condensed matter physics: frustrated spin systems[1,2], cuprates high-temperature superconductors[3–5] and strongly correlated electronic systems in general. In particular, the question of how the ISS appear as a consequence of strong electron repulsion, or spin exchange is very interesting, since the ISS come out as a result of a subtle balance between the kinetic energy loss and potential energy gain. In Ref.6, it was shown how the ISS emerge out of the on-site repulsion, at least within the mean-field approximation. On the other hand, in Refs.6–9, it was shown how an arbitrary ISS pitch vector can be treated without increasing the unit vector size by introducing the twisted boundary conditions instead of the periodic ones. It was shown therein, that at least at the mean-field level, ISS emerge as the most stable phase at the intermediate interaction strength and away from half-filling.

On the other hand, recently, our program ΘΦ[10,11], allows for ISS, superconductivity of arbitrary order and Resonating Valence Bond (RVB) states in multi-orbital electronic systems at finite temperature. In addition, ΘΦ is capable to import the hopping parameters from major *ab-initio* codes by means of WANNIER90[12] and LOBSTER[13–15] programs, which makes it possible to perform practically *ab-initio* strongly correlated magnetic or superconducting calculations.

The scope of this paper is twofold. Firstly, we test and benchmark the capabilities of ΘΦ applying it to the ISS in single orbital Hubbard model and in γ-Fe and compare our findings with those obtained previously and independently within the approaches and programs different from ΘΦ. Secondly, in this paper, we present a general framework for the spin quantization axis rotation in a general case when no assumptions are made on the spin dependence of the Hamiltonian's hopping matrix elements. This general framework extends the one already presented in the Ref.11 and allows to treat the cases when the hopping is spin-dependent and contains the spin-flip terms, thus permitting simulations of systems with spin-orbit coupling and explicit break of time-reversal symmetry.

This paper is organized as follows: we present the methods used in Sec.2 and Appendix A, the results of our ΘΦ calculations are shown in Sec.3, while Discussion and Conclusions are given in Sec.4.

METHODS

Recently proposed program ΘΦ[11] allows to fulfill two of the most important extensions of the essentially single-particle mean-field paradigm of the computational solid state physics: the admission of the Bardeen–Cooper–Schrieffer electronic ground state and allowance of the magnetically ordered states with an arbitrary superstructure (pitch) wave vector. Both features are implemented in the context of multi-band systems and permit the interface with the solid state quantum physics packages eventually providing access to the first-principles estimates of the relevant matrix elements of the model Hamiltonians derived from the standard DFT calculations. In the Ref.11, we have presented a general approach to the spin quantization axis rotation, which correctly works in the case of multi-orbital spin-independent hopping matrix elements. In the present paper, we extend the spin quantization axis rotation method to a general case of arbitrary (Hermitian) hopping. The details of the derivation are given in the Appendix A, while the brief summary is shown below:

- At a finite pitch vector $\mathbf{Q}$, a hoping matrix $t_{ij}(k,k')\delta(k-k')$ is transformed into a new matrix $\widetilde{t}_{ij}(k,k')\delta(k-k'\pm\mathbf{Q})$ in which the states with momentum k and spin e.g. "up" are connected to the states with the momentum $k+\mathbf{Q}$ and the spin "down" and vice-versa.

- The translational invariance, "broken" by imposing the incommensurate spin spiral with the pitch vector $\mathbf{Q}$, can be restored if we shift the "down" states by $\mathbf{Q}$ prior to the solution of the secular equation.
- The interaction terms like Coulomb repulsion and Heisenberg exchange, which are typically fourth rang tensors, have to be transformed according to the formulas given in Ref.11, and this task is facilitated by the fact that the most important contributions to them are local *i.e.* do not extend outside of the unit cell.
- In the case when the hopping term is spin-independent, the $\mathbf{Q}$-dependence only comes from the interaction term, and the ISS state is stabilized if the energy gain from the "spiralizing" the interaction is greater than the energy lost by the kinetic energy.
- In the case when the hopping term is spin-dependent, the kinetic energy becomes $\mathbf{Q}$-dependent, although the main contribution to the stabilization of the ISS is still expected to come from the interaction terms.

The mean-field self-consistency workflow proceeds as usual, with the modified Hamiltonian, and, at self-consistency, the internal energy $E(\mathbf{Q})$ as a function of $\mathbf{Q}$ is obtained.

RESULTS AND BENCHMARKS

Incommensurate spin spirals in Hubbard model

The single orbital Hubbard model considered in this paper has the following Hamiltonian:

$$H = -t \sum_{\langle mn \rangle} \left(c^{\dagger}_{n\sigma} c_{m\sigma} + \text{H.c.} \right) + U \sum_{n} n_{n\uparrow} n_{n\downarrow} - \mu \sum_{n\sigma} n_{n\sigma} \tag{0.1}$$

Here $c_{n\sigma}$ is the electron annihilation operator on site n with spin σ, $n_{n\sigma} = c^{\dagger}_{n\sigma} c_{n\sigma}$ is the electron occupation operator, t is the nearest neighbor hopping parameter, U is the onsite Coulomb repulsion, while μ is the chemical potential. In the Hamiltonian (0.1), the electrons move on a square lattice and only nearest neighbor hopping is considered, which is emphasized by the notation $\langle nm \rangle$. Finally, μ is the system's chemical potential, which enforces the correct number of particles in the system. The calculations are performed at a finite temperature T which was typically kept low enough ($T = 10^{-4} t$) and on a dense 2D k-point grid of 400×400 points.

The Hamiltonian (0.1) cannot be solved exactly as it is, however, in the atomic limit ($t = 0$) it does allow for the exact solution, revealing a rich phase diagram with charge and spin orderings, which rapidly evolve as a function of temperature[16–19].

In this work, we consider the incommensurate spin density waves with the pitch vector defined as:

$$\mathbf{Q} = (\pi, \pi) + \delta\,(1, 1)\,. \tag{0.2}$$

This phase is referred to as the $(1, 1)$ phase in Ref.6 and it is assumed that $\delta \ll 1$.

Within ΘΦ, the calculations are performed by using the extended density matrix ρ as the self-consistency procedure variable, so that the internal energy $E(\mathbf{Q})$ at each pitch vector $\mathbf{Q}$ is at self-consistency. In ΘΦ, the density matrix is of the most general form, allowing for incommensurate spin-density waves, superconductivity, Resonating Valence Bonds (RVB). The extended density matrix is defined through the basic fermionic operators as follows:

$$\rho_{n,m}(\tau) = \delta_{\tau,0} \delta_{n,m} - \langle \Psi^{\dagger}_{n,R} \Psi^{\dagger}_{m,R+\tau} \rangle, \tag{0.3}$$

and the operatorial basis $\Psi^{\dagger}_{R}$ for a single-orbital model is defined as:

$$\Psi^{\dagger}_{R} = \left(c^{\dagger}_{R\downarrow}, c^{\dagger}_{R\uparrow}, c^{\dagger}_{R\downarrow}, c^{\dagger}_{R\uparrow} \right). \tag{0.4}$$

In the particular case of a single band Hubbard model with spin-density waves and without superconductivity and RVB, the structure of ρ is of the following form:

$$\rho = \begin{pmatrix} \frac{n-\sigma}{2} & 0 & 0 & 0 \\ 0 & \frac{n+\sigma}{2} & 0 & 0 \\ 0 & 0 & 1 - \frac{n-\sigma}{2} & 0 \\ 0 & 0 & 0 & 1 - \frac{n+\sigma}{2} \end{pmatrix}. \tag{0.5}$$

Here, n is the average site occupation, while σ is the average site magnetization. One can see from Eq.(0.5) that this type of ρ describes a site with occupation imbalance between 'up' and 'down' channels. This would normally correspond to the ferromagnetic order, however, thanks to the method of spin quantization axis rotation, proposed in Ref.6 and 7 and implemented in ΘΦ, an arbitrary spin-density wave pitch vector can be introduced and treated at the same computational cost as the simplest ferromagnetic phase.

The multidimensional optimization built in ΘΦ (simplex algorithm) allows to optimize efficiently the internal energy of the system $E(\mathbf{Q})$ as a function of the pitch vector $\mathbf{Q}$. A typical internal energy profile and the progress of the minimization is shown in Figure1. We notice that the commensurate antiferromagnetism with the pitch vector (π, π) corresponds to a local maximum of $E(\mathbf{Q})$, and the minimum of $E(\mathbf{Q})$ is two-fold degenerate with the minima located symmetrically with respect to (π, π). The optimization procedure shown in Figure1 corresponds to a single set of the Hamiltonian parameters U and δ. We have performed a scan in this parameter

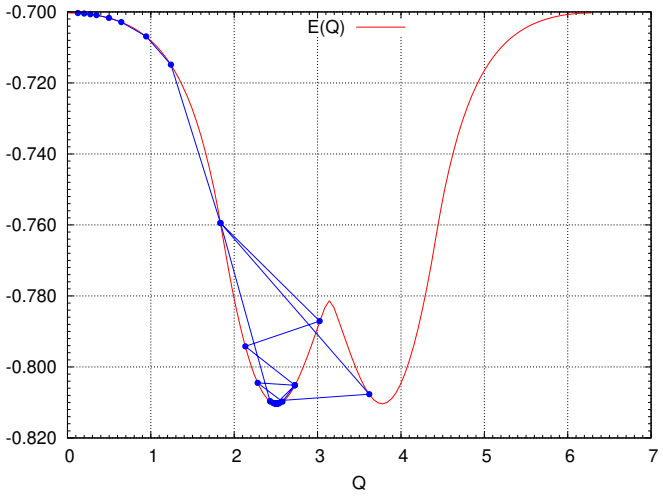

Figure 1. A typical internal energy profile $E(\mathbf{Q})$ $U = 5t$, $\delta = 0.15$, $T = 0.0001t$. $E(\mathbf{Q})$ has two local minima symmetric with respect to (π, π), which is a local maximum. The blue line shows the simplex optimization within ΘΦ.

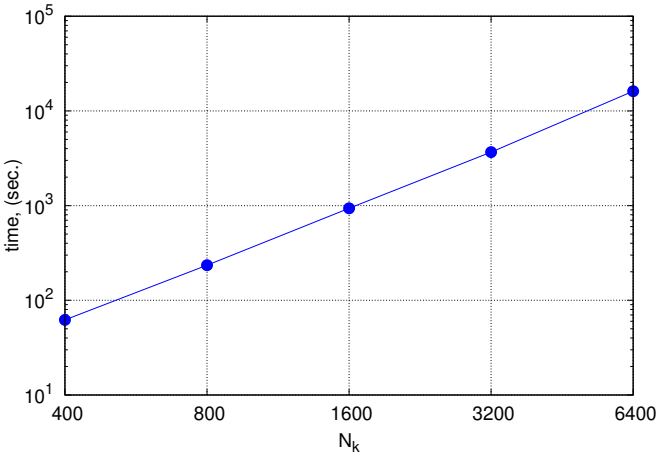

Figure 2. A benchmark of ΘΦ, showing the dependence of the time for single self-consistency solution on the number of k-points along each of the dimensions of a 2D grid in the Brillouin zone. Note the logarithmic scale on both axes. Here, N_k is the number of k-points along each of the dimensions of a 2D grid in the Brillouin zone, so that in each grid there are $N_k \times N_k$ points. $U = 10t$, $T = 0.01t$, ISS phase at $\mathbf{Q} = 0$.

space in order to benchmark our implementation against the data published in Ref.6. The comparison can be seen in Figure3. We notice a very good overall agreement between the two results which validates the use of ΘΦ in the context of ISS. At largest t/U considered ($t/U = 0.2$), the offset as a function δ starts linearly from zero and reaches saturation around $\delta = 0.25$. At a smaller value of $t/U = 0.1$ ($U = 10t$), the offset monotonically grows from zero to approximately $a\Delta\mathbf{Q}/\pi = 0.8$.

In order to demonstrate the computational efficiency of ΘΦ, we report in Figure 2 the nearly perfect scaling of our program's computational time as a function of the number of k-points in the Brillouin zone. The tests were performed for the single orbital Hubbard model on a 2D square lattice. The slope in logarithmic scale implies a quadratic dependence in the range of N_k shown, as it should be for the integration in 2D.

Spiral phases of γ-Fe

In the raw of $3d$ materials, Fe falls close to the node separating the antiferromagnetic metals Cr and Mn with a nearly half-filled d band from strong ferromagnets Co and Ni with a nearly full band. It is clear, therefore, that the magnetic ordering in Fe should be extremely sensible to the interatomic distances, bond angles, volume packing type and other crystallographic details. In fact, it was found experimentally[20], that the magnetic ordering of γ-A phase of Fe precipitates in Cu is a spin-spiral state propagating with wave vector $Q_{\text{exp}} = 2\pi/a(0.1, 0, 1)$ (Cartesian coordinates).

On the other hand, theoretically, a number of attempts has been made to tackle this problem (see Refs.13–15, and the references therein). The main theoretical conclusion was that, in general, there are two minima: one at the ΓX and the other at the XW lines, while the relative depth of these minima depends on the unit cell volume: at higher volumes, the ΓX line minimum is lower, while at lower volumes, the XW line minimum is more stable. In particular, in the Ref.21, the two minima have the following positions: $Q_1 = 2\pi/a(0, 0, 0.6)$ and $Q_2 = 2\pi/a(0.2, 0, 1)$ (Cartesian coordinates). In the internal coordinates, these points translate into: $Q_1 = \frac{6}{10}\Gamma X$, while $Q_2 = \frac{2}{5}XW$. The rational numbers in these definitions reflect the fact that the $\boldsymbol{Q}$-vector has to belong to the same finite Brillouin zone grid as the one used in the DFT calculations ($13 \times 13 \times 13$ Monkhorst-Pack in the Ref.21). Denser grids are expected to refine these numbers to some extent.

In this section, we show how this theoretical picture can be reproduced by using ΘΦ. We derive the hopping parameters from VASP DFT calculations[22] using the maximally-localized Wannier orbitals, as implemented in WANNIER90 package[12]. We consider γ-Fe with fcc lattice at several lattice constants: $a = 3.678$Å, $a = 3.583$Å, $a = 3.577$Å, $a = 3.545$Å, $a = 3.510$Å, and $a = 3.493$Å, which correspond to decreasing volumes of $V = 12.439$Å^3 $V = 11.500$Å^3, $V = 11.442$Å^3, V=11.138Å^3, $V = 10.811$Å^3 and $V = 10.655$Å^3 respectively. In extracting the hopping parameters, we utilize VASP paramagnetic DFT calculations with PBE[23] functional at a $8\times8\times8$ k-point grid, with $E = 500eV$ plane-wave cut-off. The quality of the wannierization procedure employed to obtain the hopping parameters is similar to the one reported in our previous work (Ref.11, Appendix C).

In the Refs.21, 24, and 25, the magnetic ordering originated within the LSDA approximation as a consequence of the Stoner mechanism, where the exchange correla-

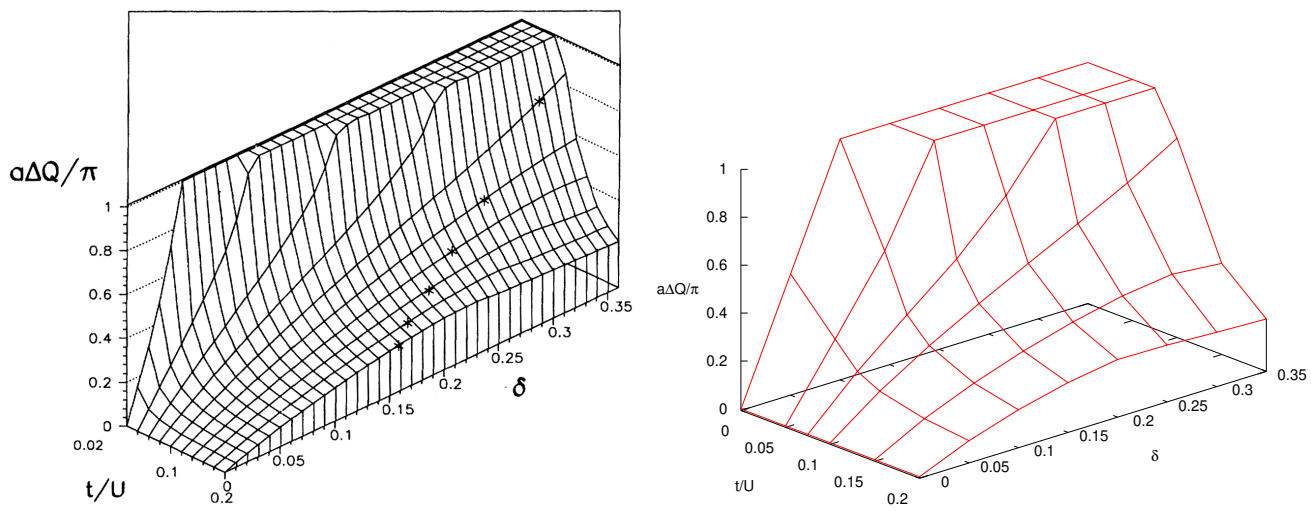

Figure 3. A benchmark of ΘΦ ISS phase diagram against the results of Ref.6: (left panel) Ref.6, (right panel) ΘΦ calculations. The axes represent inverse interaction t/U, doping δ and pitch vector offset from (π, π) normalized to π.

tion functional acts as a "driving force", gaining energy from magnetic polarization. Therefore, in this case, the exchange correlation functional determines the scale of the total energy landscape as a function of **Q**-vector. In our calculations, we use another "driving force", namely the local Heisenberg exchange interaction J which transforms under spin quantization axis rotation as described in Ref.11. This Heisenberg interaction is treated within the mean-field approach. It is clear that the scale of the relative energy gains will be of different origin in our case and cannot be directly compared to the above mentioned references. Nevertheless, we will show that the relative stability of the two local minima as a function of volume is correctly reproduced by ΘΦ. We have used $J = -1eV$ (ferromagnetic exchange) for Fe. This value was already successfully tested in our previous ΘΦ calculations of Fe in the Ref.11. In addition, this value is constrained from below by the fact that a value as small as $J = -0.8eV$ does not stabilize at all any magnetic solution, and from above by the observation that a value as big as $J = -1.2eV$ stabilizes a ferromagnetic solution, which is always more stable than any ISS state. Finally, we used a full $19 \times 19 \times 19$ Monkhorst-Pack k-point grid in our ΘΦ calculations. It was pointed out in Ref.21, that influence of the spin-orbit coupling on the magnetization in γ-Fe is very small, that is why we decided to neglect it in the present work.

Taking into account the above considerations, the Hamiltonian used in the present section assumes the form:

$$H_{\mathrm{Fe}} = \sum_{i,j,\tau,\alpha,\beta,R} c^{\dagger}_{R,i,\alpha} t^{\alpha\beta}_{ij}(\tau) c_{R+\tau,j,\beta} \qquad (0.6)$$

$$+ \sum_{i,j,\tau,\alpha,\beta,R} J^{\alpha,\beta}_{i,j}(\tau) S^{\alpha}_{i,R} S^{\beta}_{j,R+\tau}, \qquad (0.7)$$

where the hopping matrix $t^{\alpha\beta}_{ij}(\tau)$ is obtained from the wannierization procedure and is transformed under spin quantization axis rotations as described in the Appendix, $S^{\alpha}_{i,R}$ is the α-component of the spin operator on orbital i in the cell R, while the Heisenberg tensor $J^{\alpha,\beta}_{i,j}(\tau) = \delta(\tau)\delta_{\alpha,\beta} \times J$, with $J = -1eV$, and the i and j indices are restricted to the d-shell orbitals.

On the other hand, the density matrix in this case has the form summarized in TableI (only the relevant diagonal part of the particle-particle $\tau = 0$ density matrix component is show).

Here, for the sake of brevity, 18 diagonal matrix elements are arranged in a 2×9 table with the orbital indices running along the columns and the spin components running along the rows. The order of the orbitals corresponds to the one established in WANNIER90. Finally, the matrix elements are expressed in terms of the parameters n_i and m_i, so that, for example, n_s and m_s are the occupation and the magnetization of the s orbital respectively.

ΘΦ results for γ-Fe are shown in Figure 3. The total energy dependence in our calculations is, indeed, very sensible to the unit cell volume. Starting from $a = 3.493$ Å, the relative energy gain of the $\mathbf{Q}_1$ spin spiral gradually grows up to $a = 3.545$ Å, and then, as the volume increases further, starts to decrease until, at $a = 3.678$ Å, a situation realizes when the ferromagnetic state at $\mathbf{Q} = 0$ becomes the most stable. The experimental volume $V = 11.442$ Å^3, corresponding to $a = 3.577$ Å, is close to the maximum energy gain tested in the present paper: $0.1eV$. The $\mathbf{Q}_2$ spin spiral is not reproduced in our calculations in the sense that the broad minimum of the energy in the XW interval is realized at the W point or in its vicinity, although the energy difference between the $\mathbf{Q}_1$ spin spiral and the whole XW line at the experimental volume is extremely small.

Table I. Density matrix table for γ-Fe.

	s	p_z	p_x	p_y	d_{z2}	d_{xy}	d_{yz}	$d_{x^2-y^2}$	d_{xy}
$\uparrow$	$\frac{n_s+m_s}{2}$	$\frac{n_{pz}+m_{pz}}{2}$	$\frac{n_{px}+m_{px}}{2}$	$\frac{n_{py}+m_{py}}{2}$	$\frac{n_{dz2}+m_{dz2}}{2}$	$\frac{n_{dxz}+m_{dxz}}{2}$	$\frac{n_{dyz}+m_{dyz}}{2}$	$\frac{n_{dx2}+m_{dx2}}{2}$	$\frac{n_{dxy}+m_{dxy}}{2}$
	$\frac{n_s-m_s}{2}$	$\frac{n_{pz}-m_{pz}}{2}$	$\frac{n_{px}-m_{px}}{2}$	$\frac{n_{py}-m_{py}}{2}$	$\frac{n_{dz2}-m_{dz2}}{2}$	$\frac{n_{dxz}-m_{dxz}}{2}$	$\frac{n_{dyz}-m_{dyz}}{2}$	$\frac{n_{dx2}-m_{dx2}}{2}$	$\frac{n_{dxy}-m_{dxy}}{2}$

In our calculations, the d-shell magnetic moment of the spiral phase decreases as a function of $\mathbf{Q}$ at ΓX line and increases at XW line, having a minimum at X, as shown in Figure4.The absolute value of the moment, approximately one μ_B, is similar to the values reported in the Ref.21. The energy gain of the $\mathbf{Q}_1$ spin spiral phase with respect to the $\mathbf{Q} = 0$ phase is approximately twice larger than the one reported in the Refs.21 and 24, and this difference can be ascribed to a completely different mechanism which stabilizes the magnetic phase, as mentioned above.

DISCUSSION AND CONCLUSIONS

In the present paper, we have shown how ΘΦ program can be easily used to calculate the properties of incommensurate spin density waves. We have performed the benchmark of our results against those of Ref.6 and Ref.21 and shown the excellent agreement. In particular, for the single-orbital Hubbard model we have shown that the ISS state can be stabilized in a wide range of the on-site repulsion U, and the pitch vector off-set from the commensurability varies from zero to one as a function of U and doping δ. In addition, the ΘΦ minimization procedure stably locates the total energy minimum as a function of the pitch vector $\mathbf{Q}$.

In the case of the ISS in γ-Fe, we have shown that it can be successfully stabilized and has the energy lower than the ferromagnetic state, at least along the path $\Gamma \to X \to W$. Although in our calculations the interaction term, was completely different from the Refs.21 and 24 our results are rather similar to the ones reported in there. Indeed, in DFT the interaction comes from the exchange functional, which, in turn, is obtained by fitting the homogeneous electron gas Monte Carlo simulations, while in our calculations, the full (x, y, z-components) Heisenberg interaction on d-orbitals, supplied with the spin quantization axis rotation formulas was used. The only parameter in our calculations – The Heisenberg exchange J– is close to the values routinely used for iron and is constrained from below and above by the absence of magnetic solution and the instability with respect to the ferromagnetic phase respectively. Taking into account these differences, our results are in surprisingly good agreement with the previously published ones: the sensitivity to the unit cell volume, the stability of the $\mathbf{Q}_1$ state, the order of magnitude of the energy gain, the value of the magnetic moment. The only feature not reproduced in our calculations is the absolute stability of the $\mathbf{Q}_2$ state, although the energy difference between the $\mathbf{Q}_1$ and the $\mathbf{Q}_2$ states is very small. This discrepancy is currently under investigation and will be explained in a later work.

Additionally, in this paper, we have proposed a general approach for the spin quantization axis rotation of the most problematic Hamiltonian part – kinetic energy. This approach only requires the hopping matrix to be Hermitian, without demanding that the off-diagonal spin-flip terms like spin-orbit coupling be small and treated as perturbations. Such an approach will allow us to efficiently calculate the ISS in heavy elements with sizable spin-orbit coupling like lanthanides and actinides.

Within ΘΦ, both single-orbital case and a general multi-orbital one can be routinely treated as shown here and in Refs.10 and 11. This paves the way to the computationally cheap calculations of ISS in complex multi-orbital systems with the '*ab-initio*' predictive power. These calculations can be further combined with the large-scale material search codes (see *e.g.* Ref.26) in order to perform the large scale material search with the given functional properties.

Rotating the local quantization axes

In this Appendix, we briefly review the method of local quantization axes rotation, originally formulated in Refs.6, 8, 9, 11, and 27.

The most general form of spin-dependent hopping between an orbital i and an orbital j is:

$$t_{ij}(\tau) = \begin{pmatrix} t_{ij}^{\uparrow\uparrow}(\tau) & t_{ij}^{\uparrow\downarrow}(\tau) \\ t_{ij}^{\downarrow\uparrow}(\tau) & t_{ij}^{\downarrow\downarrow}(\tau) \end{pmatrix}. \tag{8}$$

It obeys the hermiticity condition:

$$t_{ij}(\tau) = t_{ji}^{\dagger}(-\tau).$$

On the other hand, the rotation operator (around y-axis) reads as:

$$\Omega_\tau = e^{-i\frac{(\mathbf{Q},\tau)}{2}\sigma_y}.$$

Here, we rotate the spin-quantization axes around y-axis, that is why σ_y appears in Ω_τ. The other choices would be rotations around x- and z-axis and could be simply accounted for by substituting $y \to x$ or $y \to z$.

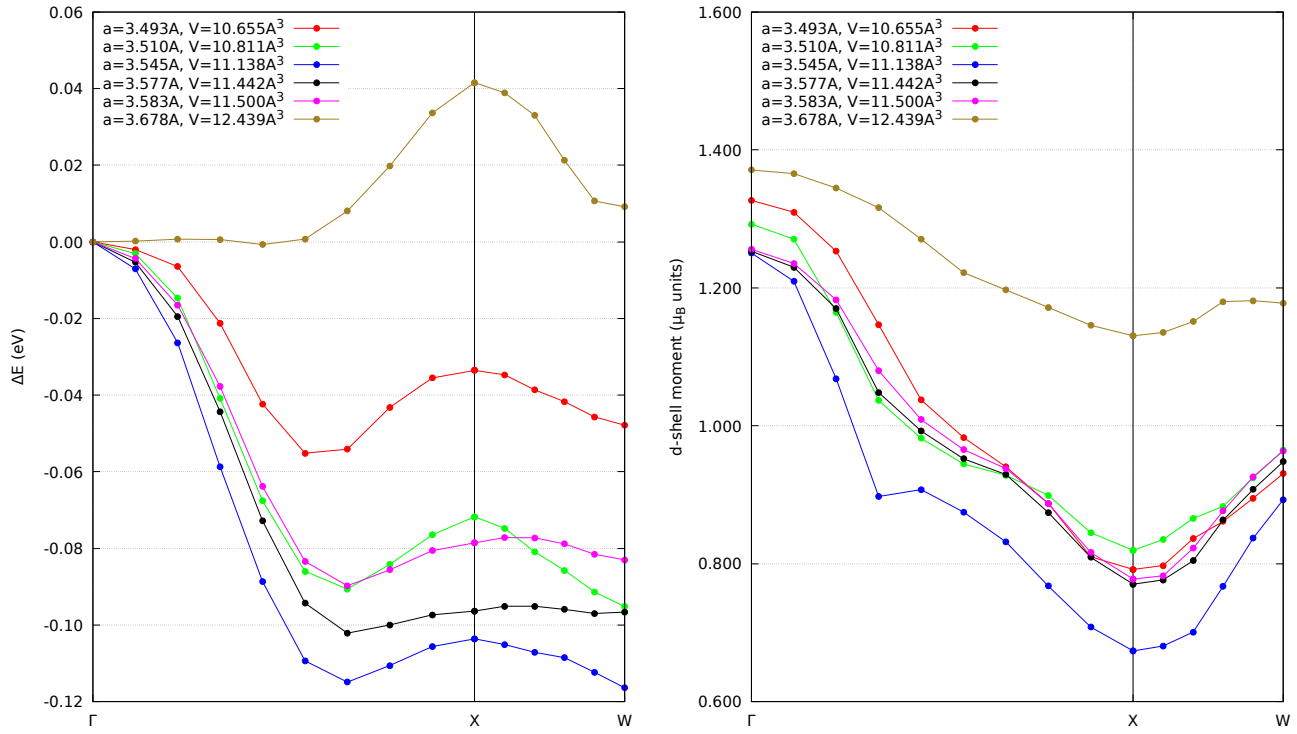

Figure 4. Left panel: A scan on pitch vector along the $\Gamma \to X \to W$ path of the spin spiral state energy gain with respect to the ferromagnetic state for different unit cell volumes to compare against the results of Ref.21. Right panel: The total d-shell magnetization along the same path for different volumes. The black lines correspond to the experimental volume.

For the moment, we leave apart the individual orbital rotations Ω_i (which are also implemented in $\Theta\Phi$) since they do not interfere with the lattice translations, and we will take them into account in the final answer. The rotated-by-the-super-structure-vector-$\mathbf{Q}$ kinetic energy reads as:

$$\widetilde{T} = \sum_{i,j,\tau,\alpha,\beta,R} c^{\dagger}_{R,i,\alpha} \left(e^{i\frac{(\mathbf{Q},R)}{2}\sigma_y} t_{ij}(\tau) e^{-i\frac{(\mathbf{Q},(R+\tau))}{2}\sigma_y} \right)_{\alpha,\beta} c_{R+\tau,j,\beta}. \tag{9}$$

We convert the summation on R into the summation on k and k':

$$\widetilde{T} = \frac{1}{N} \sum_{i,j,\tau,\alpha,\beta,R,k,k'} e^{-ik'\tau} e^{i(k-k')R} c^{\dagger}_{k,i,\alpha} \tag{10}$$

$$\times \left(e^{i\frac{(\mathbf{Q},R)}{2}\sigma_y} t_{ij}(\tau) e^{-i\frac{(\mathbf{Q},(R+\tau))}{2}\sigma_y} \right)_{\alpha,\beta} c_{k',j,\beta} \tag{11}$$

If we define the matrix $L_{ij}(k-k',\tau)$:

$$L_{ij}(k-k',\tau) = \frac{1}{N} \sum_{R} e^{i(k-k')R} e^{i\frac{(\mathbf{Q},R)}{2}\sigma_y} t_{ij}(\tau) e^{-i\frac{(\mathbf{Q},R)}{2}\sigma_y}, \tag{12}$$

then the kinetic energy expression simplifies as follows:

$$\widetilde{T} = \sum_{i,j,\tau,\alpha,\beta,k,k'} e^{-ik'\tau} c^{\dagger}_{k,i,\alpha} L_{ij}(k-k',\tau) e^{-i\frac{(\mathbf{Q},\tau)}{2}\sigma_y} c_{k',j,\beta} \tag{13}$$

$$= \sum_{i,j,\tau,\alpha,\beta,k,k'} e^{-ik\tau} c^{\dagger}_{k,i,\alpha} e^{-i\frac{(\mathbf{Q},\tau)}{2}\sigma_y} L_{ij}(k-k',\tau) c_{k',j,\beta}.$$

Let us consider the matrix $L_{ij}(k-k',\tau)$. First of all, if the matrix $t_{ij}(\tau)$ is proportional to identity, or to σ_y then the rotations on the left and right hand side cancel each other and $L_{ij}(k-k',\tau) = \delta(k-k')t_{ij}(\tau)$ and we obtain the result outlined in the Ref.11. Although, there is still a room for the non-trivial results, the most physically interesting situation is when $t_{ij}(\tau)$ does not commute with σ_y, spin-orbit coupling being an important example. In the general case, we can write:

$$\Omega_\tau = \cos\frac{(\mathbf{Q},\tau)}{2} - i\sigma_y \sin\frac{(\mathbf{Q},\tau)}{2},$$

so that after some simplification we have:

$$L_{ij}(k-k',\tau) = \frac{1}{2N}\sum_R e^{i(k-k')R} \times \{t_{ij}(\tau) + \sigma_y t_{ij}(\tau)\sigma_y + (t_{ij}(\tau) - \sigma_y t_{ij}(\tau)\sigma_y)\cos(\mathbf{Q},R) + i\,[\sigma_y, t_{ij}(\tau)]\sin(\mathbf{Q},R)\}\,. \tag{14}$$

At this point, we can do the Fourier transform in the above expression, but the problem now is that the resulting expression will not be diagonal in k-space, *i.e.* there will be terms with k and $k \pm \mathbf{Q}$ connected!

Till now, the formalism is completely general and other cases of rotation around *e.g.* x or y axes can be performed by substituting $y \to x$, or $y \to z$. The case of rotation around z axis is particularly instructive since σ_z is diagonal. In the most general case we can present:

$$t_{ij}(\tau) = \begin{pmatrix} a_{ij}(\tau) & c_{ij}(\tau) \\ d_{ij}(\tau) & b_{ij}(\tau) \end{pmatrix} = t_{ij}^{\parallel} + t_{ij}^{\perp} \tag{15}$$

$$= \begin{pmatrix} a_{ij}(\tau) & 0 \\ 0 & b_{ij}(\tau) \end{pmatrix} + \begin{pmatrix} 0 & c_{ij}(\tau) \\ d_{ij}(\tau) & 0 \end{pmatrix}. \tag{16}$$

The first matrix will commute with σ_z and will only contribute to the first term (independent on $\mathbf{Q}$) in $L_{ij}(k-k',\tau)$. For $t_{ij}^{\perp}$ we can explicitly work out:

$$\sigma_z t_{ij}^{\perp}(\tau)\sigma_z = -t_{ij}^{\perp}(\tau) \tag{17}$$

$$\left[\sigma_z, t_{ij}^{\perp}(\tau)\right] = 2\begin{pmatrix} 0 & c_{ij}(\tau) \\ -d_{ij}(\tau) & 0 \end{pmatrix}. \tag{18}$$

Therefore, $L_{ij}(k-k',\tau)$ will become:

$$L_{ij}(k-k',\tau) = t_{ij}^{\parallel}(\tau)\delta(k-k') + t_{ij}^{\perp}(\tau)\begin{pmatrix} \delta(k-k'-\mathbf{Q}) & 0 \\ 0 & \delta(k-k'+\mathbf{Q}) \end{pmatrix}. \tag{19}$$

At this point we can introduce the Fourier transforms:

$$\sum_\tau t_{ij}(\tau)e^{-ik\tau} = \begin{pmatrix} a_{ij}(k) & c_{ij}(k) \\ c_{ij}^\star(k) & b_{ij}(k) \end{pmatrix},$$

where we have used the hermiticity condition:

$$\sum_\tau d_{ij}(\tau)e^{-ik\tau} = \sum_\tau c_{ij}^\star(-\tau)e^{-ik\tau}.$$

Substituting $L_{ij}(k-k',\tau)$ into Eq.(13) and changing $\sigma_y \to \sigma_z$, we obtain, after simplifications:

$$\widetilde{T}_z(\mathbf{Q}) = \sum_{i,j,k}\left(c_{k,i,\uparrow}^\dagger, c_{k+\mathbf{Q},j,\downarrow}^\dagger\right) \times \tag{20}$$

$$\begin{pmatrix} a_{ij}(k+\frac{\mathbf{Q}}{2}) & c_{ij}(k+\frac{\mathbf{Q}}{2}) \\ c_{ij}^\star(k+\frac{\mathbf{Q}}{2}) & b_{ij}(k+\frac{\mathbf{Q}}{2}) \end{pmatrix}\begin{pmatrix} c_{k,i,\uparrow} \\ c_{k+\mathbf{Q},j,\downarrow} \end{pmatrix}. \tag{21}$$

The rotation around y-axis can be evaluated similarly, although the calculations in that case are more cumbersome. We report below the final answer:

$$\widetilde{T}_y(\mathbf{Q}) = \sum_{i,j,k}\left(c_{k,i,\uparrow}^\dagger, c_{k+\mathbf{Q},j,\downarrow}^\dagger\right) \times \tag{22}$$

$$\begin{pmatrix} \alpha_{ij}(k+\frac{\mathbf{Q}}{2}) & \gamma_{ij}(k+\frac{\mathbf{Q}}{2}) \\ \gamma_{ij}^\star(k+\frac{\mathbf{Q}}{2}) & \beta_{ij}(k+\frac{\mathbf{Q}}{2}) \end{pmatrix}\begin{pmatrix} c_{k,i,\uparrow} \\ c_{k+\mathbf{Q},j,\downarrow} \end{pmatrix}. \tag{23}$$

where:

$$\alpha_{ij}(k) = \frac{a_{ij}(k)+b_{ij}(k)}{2} + \mathrm{Im}\, c_{ij}(k) \tag{24}$$

$$\beta_{ij}(k) = \frac{a_{ij}(k)+b_{ij}(k)}{2} - \mathrm{Im}\, c_{ij}(k) \tag{25}$$

$$\gamma_{ij}(k) = -\frac{a_{ij}(k)+b_{ij}(k)}{2} - i\mathrm{Re}\, c_{ij}(k) \tag{26}$$

It is easy to see that $\widetilde{T}_z(\mathbf{Q})$ and $\widetilde{T}_y(\mathbf{Q})$ are different representations of the same operator and, indeed, are related by a unitary transformation S:

$$S = \frac{1}{\sqrt{2}}\begin{pmatrix} i & -i \\ 1 & 1 \end{pmatrix},$$

so that:

$$S^\dagger \begin{pmatrix} a_{ij}(k) & c_{ij}(k) \\ c_{ij}^\star(k) & b_{ij}(k) \end{pmatrix} S = \begin{pmatrix} \alpha_{ij}(k) & \gamma_{ij}(k) \\ \gamma_{ij}^\star(k) & \beta_{ij}(k) \end{pmatrix}.$$

It can be seen, that the two ways to rotate the quantization axis are fully equivalent. Since rotation around z-axis features somehow simpler formulas, we will carry out further calculations assuming z-axis rotation.

Putting back the individual orbital rotations Ω_i, we can assemble the final rotation formula for the multi-orbital case as follows:

$$\widetilde{T}_z(\mathbf{Q}) = \sum_{i,j,k} \left(c^\dagger_{k,i,\uparrow}, c^\dagger_{k+\mathbf{Q},j,\downarrow} \right) \Omega^\dagger_i \begin{pmatrix} a_{ij}(k+\frac{\mathbf{Q}}{2}) & c_{ij}(k+\frac{\mathbf{Q}}{2}) \\ c^\star_{ij}(k+\frac{\mathbf{Q}}{2}) & b_{ij}(k+\frac{\mathbf{Q}}{2}) \end{pmatrix} \Omega_j \begin{pmatrix} c_{k,i,\uparrow} \\ c_{k+\mathbf{Q},j,\downarrow} \end{pmatrix}. \quad (27)$$

In this formula, the states with different k-vectors are mixed. This breaks the translational invariance of the crystal and makes it impossible to effectively treat ISS states. The way out of this situation is to shift the down-spin electronic states by the vector $\mathbf{Q}$ so that in the new notation the Fockian matrix will be diagonal in k-space:

$$\widetilde{T}_z(\mathbf{Q}) = \sum_{i,j,k} \left(c^\dagger_{k,i,\uparrow}, \widetilde{c}^\dagger_{k,j,\downarrow} \right) \Omega^\dagger_i \times \quad (28)$$

$$\begin{pmatrix} a_{ij}(k+\frac{\mathbf{Q}}{2}) & c_{ij}(k+\frac{\mathbf{Q}}{2}) \\ c^\star_{ij}(k+\frac{\mathbf{Q}}{2}) & b_{ij}(k+\frac{\mathbf{Q}}{2}) \end{pmatrix} \Omega_j \begin{pmatrix} c_{k,i,\uparrow} \\ \widetilde{c}_{k,j,\downarrow} \end{pmatrix}, \quad (29)$$

where $\widetilde{c}_{k,j,\downarrow} = c_{k+\mathbf{Q},j,\downarrow}$.

For what regards the interaction term, we consider here only the generalized Heisenberg term, as defined in the Ref.11:

$$H_J = \sum_{i,j,R,\tau,\alpha,\beta} J^{\alpha,\beta}_{i,j}(\tau) S^\alpha_{i,R} S^\beta_{j,R+\tau},$$

where $S^\alpha_{i,R} = \frac{1}{2}\sum_{s,s'} c^\dagger_{R,i,s}\sigma^\alpha_{s,s'}c^\dagger_{R,i,s'}$ is the operator of the α-s component of the spin of the orbital i in the cell R. The transformation of the exchange coupling $J^{\alpha,\beta}_{i,j}(\tau)$ under the spin quantization axis rotation is reported in the Ref.11.

* evgeny.plekhanov@kcl.ac.uk

[1] A. A. Nersesyan, A. O. Gogolin, and F. H. Eßler, Physical Review Letters **81**, 910 (1998).
[2] E. Plekhanov, A. Avella, and F. Mancini, Physical Review B **74**, 115120 (2006).
[3] T. R. Thurston, R. J. Birgeneau, M. A. Kastner, N. W. Preyer, G. Shirane, Y. Fujii, K. Yamada, Y. Endoh, K. Kakurai, M. Matsuda, Y. Hidaka, and T. Murakami, Physical Review B **40**, 4585 (1989).
[4] E. Plekhanov, A. Avella, F. Mancini, and F. P. Mancini, Journal of Physics: Conference Series **273**, 012147 (2011).
[5] A. Avella, F. Mancini, F. P. Mancini, and E. Plekhanov, Journal of Physics: Conference Series **273**, 012091 (2011).
[6] E. Arrigoni and G. C. Strinati, Physical Review B **44**, 7455 (1991).
[7] O. N. Mryasov, A. I. Liechtenstein, L. M. Sandratskii, and V. A. Gubanov, Journal of Physics: Condensed Matter **3**, 7683 (1991).
[8] L. M. Sandratskii, Journal of Physics: Condensed Matter **3**, 8565 (1991).
[9] L. M. Sandratskii, Journal of Physics: Condensed Matter **3**, 8587 (1991).
[10] E. A. Plekhanov and A. L. Tchougréeff, in *Handbook of Solid State Chemistry* (Wiley-VCH Verlag GmbH & Co. KGaA, Weinheim, Germany, 2017) p. 87.
[11] E. Plekhanov, A. Tchougréeff, and R. Dronskowski, Computer Physics Communications **251**, 107079 (2020).
[12] A. A. Mostofi, J. R. Yates, Y. S. Lee, I. Souza, D. Vanderbilt, and N. Marzari, Computer Physics Communications **178**, 685 (2008).
[13] V. L. Deringer, A. L. Tchougréeff, and R. Dronskowski, Journal of Physical Chemistry A **115**, 5461 (2011).
[14] S. Maintz, V. L. Deringer, A. L. Tchougréeff, and R. Dronskowski, Journal of Computational Chemistry **37**, 1030 (2016).
[15] A. L. Tchougréeff and R. Dronskowski, Journal of Physical Chemistry A **117**, 7980 (2013).
[16] F. Mancini, E. Plekhanov, and G. Sica, Central European Journal of Physics **10**, 609 (2012).
[17] F. Mancini, E. Plekhanov, and G. Sica, The European Physical Journal B **86**, 408 (2013).
[18] F. Mancini, E. Plekhanov, and G. Sica, Journal of Physics: Conference Series **391**, 012148 (2012).
[19] F. Mancini, E. Plekhanov, and G. Sica, The European Physical Journal B **86**, 224 (2013).
[20] Y. Tsunoda, Journal of Physics: Condensed Matter **1**, 10427 (1989).
[21] M. Marsman and J. Hafner, Physical Review B **66**, 1 (2002).
[22] D. Kresse, G. Joubert, Physical Review B **59**, 1758 (1999).
[23] J. P. Perdew, K. Burke, and M. Ernzerhof, Physical Review Letters **77**, 3865 (1996).
[24] K. Knöpfle, L. M. Sandratskii, and J. Kübler, Physical Review B **62**, 5564 (2000).
[25] D. Bylander and L. Kleinman, Physical Review B **58**, 9207 (1998).
[26] A. R. Oganov and C. W. Glass, Journal of Chemical Physics **124**, 244704 (2006).
[27] C. Barreteau, D. Spanjaard, and M. C. Desjonquéres, Comptes Rendus Physique **17**, 406 (2016).